PNAS RESEARCH ARTICLE | PLANT BIOLOGY OPEN ACCESS

# Proviral insights of glycolytic enolase in *Bamboo mosaic virus* replication associated with chloroplasts and mitochondria

Kuan-Yu Lin[a], Ying-Wen Huang[b,c], Liang-Yu Hou[a], Hsin-Chuan Chen[a], Yu Wu[a], I-Hsuan Chen[b,c], Ying-Ping Huang[b,c], Shu-Chuan Lee[a], Chung-Chi Hu[b], Ching-Hsiu Tsai[b], Yau-Heiu Hsu[b,c], and Na-Sheng Lin[a,b,1]

Affiliations are included on p. 11.

Edited by John Coffin, Tufts University, Boston, MA; received July 31, 2024; accepted March 20, 2025

**Diverse single-stranded RNA viruses employ different host cellular organelles or membrane systems to compartmentalize their replication intermediates and proviral factors, ensuring robust replication. Replication of *Bamboo mosaic virus* (BaMV), an *Alphaflexiviridae* family, is tightly associated with chloroplasts and dynamic cytosolic viral replication complex (VRC) clusters. BaMV VRC clusters comprise double-stranded viral RNA, BaMV replicase ($Rep_{BaMV}$), and mitochondrial outer membrane protein, voltage-dependent anion channel (VDAC). In this study, we demonstrate that host glycolytic enolase (ENO) binds to untranslated regions of BaMV RNA independently of ENO hydrolytic activity. However, the structural integrity of ENO is essential for its direct interaction with $Rep_{BaMV}$, and its positive regulating role in BaMV replication and the size of BaMV VRC clusters. Additionally, ENO, pyruvate kinase (PYK), and VDAC colocalize within cytosolic BaMV VRC clusters embedded in the convoluted endomembrane reticulum (ER) along with ER-targeted viral movement proteins under BaMV infection. This association suggests that the ENO-PYK-VDAC metabolon, with ENO serving as a scaffold to link chloroplasts and mitochondria, may play a pivotal role in BaMV robust replication. Collectively, our findings offer significant insights into how glycolytic ENO acts in BaMV replication.**

enolase | viral replication complex | *Bamboo mosaic virus* | chloroplast-mitochondria association

## Significance

Viruses are obligate parasites that often use internal membranous structures to create environments enriched with host factors, providing a protection environment for replication. Previous evidence shows that *Bamboo mosaic virus* (BaMV) hijacks nucleus-encoded chloroplast proteins for RNA targeting to chloroplasts and for subgenomic RNA transcription within chloroplasts. Moreover, it recruits several cytoplasmic proteins and mitochondria outer membrane protein, voltage-dependent anion channel (VDAC) into BaMV replication complex, which is essential for its replication. In this study, we identified pivotal role of the glycolytic enzyme enolase (ENO) in BaMV replication by maintaining ENO-VDAC metabolon, which depends on ENO structural integrity, and connects the chloroplasts and mitochondria. Our findings reveal that BaMV replication requires dynamic and sequential interactions between these two intracellular organelles.

Viruses are obligate parasites that commandeer host proteins, cellular machineries, metabolic resources, and internal membranous structures to accomplish their replication and dissemination. Virus infection is a dynamic process that causes host cell spatiotemporal reorganization for replication and intracellular trafficking. Diverse membrane systems, such as endoplasmic reticulum (ER), mitochondria, chloroplasts, tonoplasts, vacuoles, Golgi apparatus, peroxisomes, and plasma membrane are used by *Tombusviruses*, *Tobamoviruses*, *Hordeiviruses*, *Potyviruses,* and *Potexviruses* as viral replication organelles (VRO) (1–3) or to form viral replication complexes (VRCs) to support robust virus replication through interactions between host proteins and versatile viral proteins or viral RNA (1, 4–6). Diverse host factors (HFs) within the VRC are recruited from different organelles, and the VRC changes their form and constituents over time during virus replication and intracellular movement. Thus, how viruses utilize cell (endo)membrane systems and enable interorganelle communication to establish a VRC enriched in host proviral factors that can shield their double-stranded RNA replication intermediates from the host RNA silencing surveillance system is an engrossing question.

Virus infection not only alters the host metabolism to generate energy and macromolecules beneficial for viral propagation, but also physically hijacks metabolic enzymes into virions and the VRC. For example, Dengue virus (DENV) N3 protein interacts with fatty acid synthase to regulate DENV VRC formation (7); *Tomato bushy stunt virus* (TBSV) replicase proteins P92 and P33 recruit glyceraldehyde 3-phosphate dehydrogenase (GAPDH), fructose-bisphosphate aldolase, and enolase (ENO) to stimulate plus-strand synthesis by generating ATP-enriched compartments (8–10); and *Rice dwarf virus* Pns11 protein, a component of viroplasm, interacts with S-adenosyl-L-methionine synthetase (SAMS) to increase ethylene production for plant counterdefense (11). Notably, host-encoded ENO is also packed into virions (12), but it plays an antiviral role in HIV infection (13) and prevents HIV-1 integration (14).

ENO is a ubiquitous and conserved $Mg^{2+}$-bound metalloenzyme that catalyzes the reversible conversion of 2-phosphoglycerate (2-PG) to phosphoenolpyruvate (PEP) in the glycolysis pathway (15). In plants, glycolysis primarily takes place in the cytosol, as well as in some plastids of nonphotosynthetic tissues, mediated by various isozymes (16). It is a multifunctional protein, acting as an enzyme, scaffold, chaperone, receptor (15), and HF for

The authors declare no competing interest.

This article is a PNAS Direct Submission.



[1]To whom correspondence may be addressed. Email: nslin@sinica.edu.tw.

This article contains supporting information online at https://www.pnas.org/lookup/suppl/doi:10.1073/pnas.2415089122/-/DCSupplemental.

Published May 6, 2025.

*Hepatitis B virus* (HBV) (17) and TBSV (8) replication. As a positive regulator of both HBV and TBSV, it suppresses the interferon signaling pathway (17) or cooperates with several ATP-generating glycolytic enzymes to form a VRO (8). Furthermore, ENO also regulates immune responses in *Arabidopsis thaliana* (18).

*Bamboo mosaic virus* (BaMV) is a single-stranded positive-sense RNA virus belonging to the genus *Potexvirus* of the family *Alphaflexiviridae* (19). There are five open reading frames (ORFs) in the BaMV genome, which encode a replicase ($Rep_{BaMV}$) harboring functional domains with methyltransferase (20, 21), a helicase (22), and RNA-dependent RNA polymerase (23) activities for viral replication, three overlapping triple gene block proteins (TGBps) for movement (24–26), and a capsid protein (CP) for encapsidation (27), movement (28), and symptom formation (29), respectively. Several HFs involved in BaMV replication have been identified either through their binding to its 3′ untranslated region (UTR) or their interaction with $Rep_{BaMV}$ (30–33). BaMV co-opts chloroplastic phosphoglycerate kinase (chPGK) for targeting viral RNA to chloroplasts (34) and thylakoid-resident photosystem II oxygen-evolving complex protein (PsbO1) for subgenomic RNA transcription (35). BaMV also induces autophagy-related gene 8 (ATG8) and $Rep_{BaMV}$-enriched vesicles possibly derived from chloroplasts for proviral replication (36). The S100 membranous fraction of BaMV-infected cells exhibits replicase activity and consists of TGBps, CP, virions and mitochondrial outer membrane protein, and voltage-dependent anion channel proteins (VDACs), indicating BaMV replication is associated with mitochondria in cytosol (37, 38). Moreover, this cytosolic BaMV VRC partially colocalizes with ER and moves within cells as a mobile VRC (mVRC) (38). Therefore, BaMV may utilize multiple cellular membranous systems for its replication and intracellular movement to complete its infection cycle.

Here, we have identified ENO as an RNA binding protein (RBP) that binds to the UTR of BaMV RNA and that its hydrolase activity is essential for cytosolic VRC formation and for BaMV replication. Using confocal microscopy, we observed that ENO, pyruvate kinase (PYK), and VDAC colocalizes with the cytosolic BaMV VRC clusters near chloroplasts and enriched with mitochondria, along with movement proteins (MPs) and CP associated with ER. Given that a glycolysis metabolon consisting of phosphoglycerate mutase (PGM), ENO, pyruvate kinase (PYK), and VDAC is responsible for chloroplast-mitochondria association (39), we identified ENO as a critical HF that links chloroplasts and mitochondria and assists in the formation of the VRC clusters embedded in ER for BaMV robust replication.

## Results

**Identification of HFs Recruited by the BaMV 5′ UTR.** Previously, HFs contributing to BaMV replication were extensively revealed via binding assay to the BaMV 3′ UTR or to crude BaMV replication complex (30). Here, we used the 5′ UTR of BaMV as a probe to identify HFs potentially involved in replication. In brief, in vitro transcripts of the 5′ UTR of BaMV were fused with streptomycin-binding aptamers (StreptoTag) (40) to isolate host RBPs from crude cell extract of evacuolated BY2 protoplasts (41). These RBPs were separated on SDS-PAGE, silver-stained, and subjected to liquid chromatography-mass spectrometry (LC/MS). Apart from previously known HFs bound to the BaMV 3′ UTR, e.g. heat shock protein 90 (Hsp90) (42), PGK (43), GAPDH (44), and eEF1A (34), we also detected ENO and PGM in this assay (*SI Appendix*, Fig. S1). For further analysis, we cloned full-length ENO from *Nicotiana benthamiana* (*SI Appendix*, Fig. S2), which is an ortholog of *Phyllostachys edulis* ENO (GenBank: FP092434.1) and *AtENO2*.

To assay if ENO directly binds to the BaMV 5′ UTR, we performed electrophoretic mobility shift assay (EMSA). By EMSA using serial amounts of purified recombinant ENO-His tagged (rENO) protein, we detected band shifts of $^{32}$P-labeled BaMV 5′ and 3′ UTRs when incubated with ~1 μg WT rENO protein (Fig. 1*A*). However, an unrelated *Cucumber mosaic virus* (CMV) 3′ UTR probe rarely bound to rENO, and CMV 5′ UTR probe did not bind to rENO even when incubated with up to 4 μg rENO protein (Fig. 1*A*). The binding affinity of rENO to BaMV 5′ UTR is higher than its affinity for the BaMV and CMV 3′ UTRs by competitive EMSA (*SI Appendix*, Fig. S3*A*). Thus, rENO WT exhibits an RNA-binding capability for the UTRs of BaMV but rarely to CMV.

Previously, we successfully isolated a partially purified membrane-bound fraction (P30) from BaMV-infected *N. benthamiana* leaves that can fully support replication in vitro of BaMV and its associated satellite RNA, satBaMV, assigned as a "BaMV RdRp preparation" (45). Although $Rep_{BaMV}$ could not be detected per se in BaMV RdRp preparation by protein blot, likely due to limited levels, it is noteworthy that $Rep_{BaMV}$ levels could be enhanced by coexpressing satBaMV to function as an RNA scaffold (46). To determine whether ENO interacts with $Rep_{BaMV}$ in BaMV RdRp preparation, we performed a coimmunoprecipitation assay on ENO-DsRed-overexpressing WT and $Rep_{BaMV}$ transgenic *N. benthamiana* (O1) that was able to support satBaMV replication (31). By immunoprecipitation with ENO antibody, we detected $Rep_{BaMV}$ in the P30 fraction of BaMV RdRp preparation from $Rep_{BaMV}$ transgenic plants infiltrated with *Agrobacterium* harboring pKF4 (the infectious cDNA clone of satBaMV) (47), but not from WT plants (Fig. 1*B*). This result indicates that ENO interacts with $Rep_{BaMV}$ primarily in BaMV RdRp preparation.

**ENO Is Essential for Efficient BaMV Replication.** To elucidate further if ENO affects BaMV replication, we used *Tobacco rattle virus* (TRV)-based virus-induced gene silencing (VIGS) technology to knock down ENO in *N. benthamiana*. Plants infiltrated with a GFP construct were used as a negative control. GFP- and ENO-silenced systemic leaves were harvested at 7 dpa for protoplast isolation. Reverse transcription-qPCR (RT-qPCR) revealed an 80% reduction of ENO in the ENO-silenced protoplasts relative to GFP-silenced protoplasts at 7 dpa (Fig. 2*A*). Next, we infected GFP- and ENO-silenced protoplasts with BaMV and harvested them at 24 hours-post-inoculation (hpi). RNA blotting demonstrated that levels of the genomic and two subgenomic (sgRNA1 and sgRNA2) RNAs of BaMV were dramatically reduced in ENO-silenced protoplasts to 20% of those in GFP-silenced protoplasts (Fig. 2*B*).

We further assessed whether ENO is a general regulator for RNA virus replication. To do so, we challenged GFP- and ENO-silenced protoplasts with another Potexvirus, *Potato virus X* (PVX), and two other representative viruses, i.e., *Tobacco mosaic virus* (TMV) of Genus *Tobamovirus* and CMV of Genus *Cucumovirus*. Similar to the significant reduction observed for BaMV levels (Fig. 2*B*), we detected a ~60% reduction in PVX level in ENO-knockdown protoplasts (Fig. 2*C*). In contrast, ENO silencing had no obvious effect on TMV or CMV accumulation (Fig. 2 *D* and *E*). This indicates that the regulatory role of ENO in viral replication is specific to *Potexviruses*, with less effect observed in PVX.

To further confirm the role of ENO in BaMV replication, we performed an ENO overexpression assay. Vectors overexpressing GFP or ENO-HA fusion proteins were coinfiltrated with pKB, a BaMV infectious clone (47), into *N. benthamiana* leaves. At 3 dpa, overexpressed ENO-HA was detected by protein blot using anti-HA antibody (Fig. 2*F*). In ENO-HA-overexpressing leaves, BaMV levels increased to ~1.5-fold those of GFP-expressing leaves, as

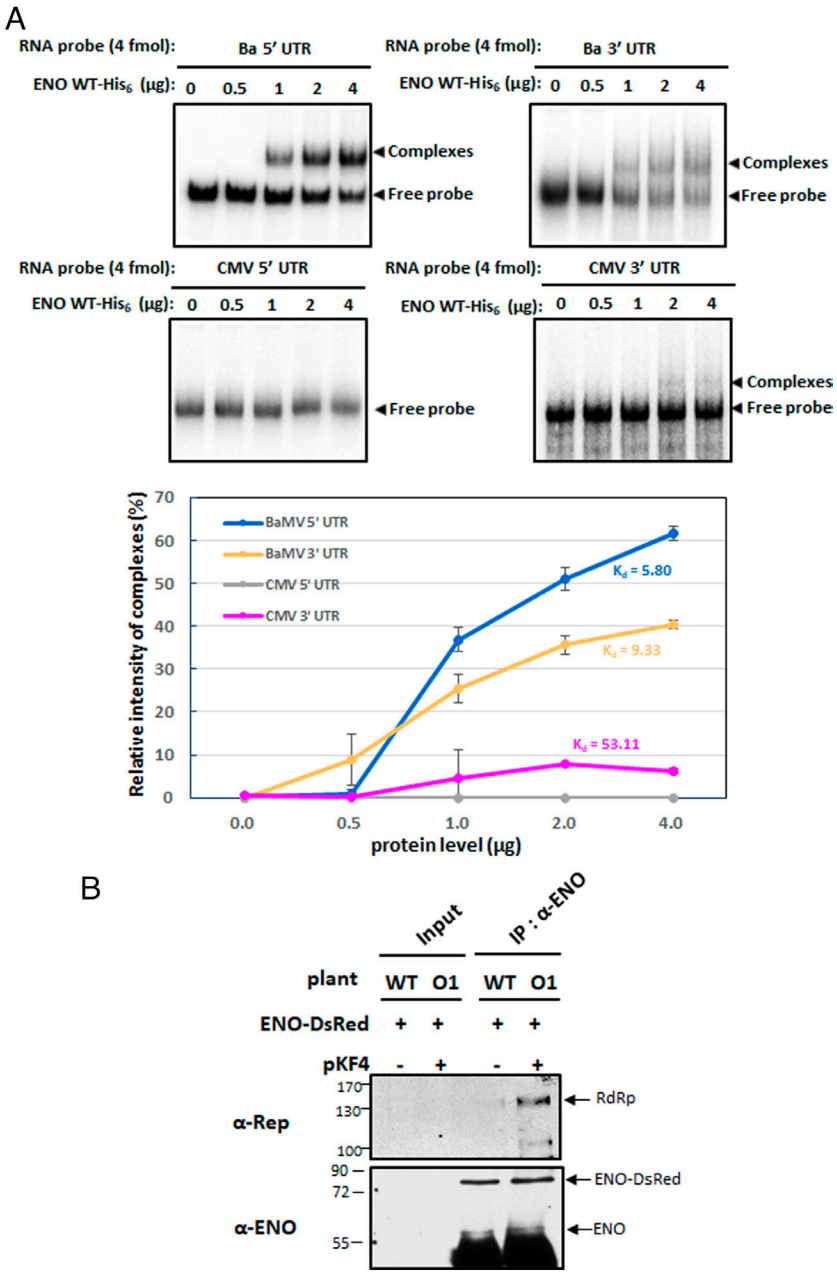


**Fig. 1.** Enolase (ENO) is a BaMV 5′ UTR binding protein that interacts with $Rep_{BaMV}$ by EMSA analysis and coimmunoprecipitation assay. (*A*) RNA binding activity of different amount of recombinant ENO wild-type (WT) protein incubated with 5′ UTR of BaMV (Ba 5′ UTR), CMV (CMV 5′ UTR), and 3′ UTR of BaMV (Ba 3′ UTR) and CMV (CMV 3′ UTR) was assayed by EMSA. (*B*) Interaction of ENO and $Rep_{BaMV}$ in satBaMV replication fraction. P30 fraction of ENO-DsRed infiltrated WT *N. benthamiana* leaves (WT) or ENO-DsRed and pKF4 coinfiltrated $Rep_{BaMV}$ transgenic *N. benthamiana* leaves (O1) at 2 days-post-agroinfiltration (dpa) were purified and immunoprecipitated by ENO antiserum. After immunoprecipitation, $Rep_{BaMV}$ and ENO were detected by protein blot. O1: $Rep_{BaMV}$ transgenic *N. benthamiana.*

determined by RNA blot (Fig. 2*G*). These results clearly demonstrate that ENO is required for facilitating BaMV replication.

**ENO's Enzymatic Function Is Involved in BaMV Replication.** ENO forms a homodimer that converts 2-PG into PEP in the glycolysis pathway. By comparing ENO from *N. benthamiana* with previously characterized ENO from sunflower (*Helianthus annuus* L.) (48), we predicted residues important for ENO activity, including substrate binding, dimer formation, and $Mg^{2+}$ binding. Accordingly, we conducted site-directed mutagenesis to generate respective *eno* mutants: ENO S42A ($Mg^{2+}$-binding domain), ENO H380A (substrate-binding domain), and ENO TM (a $Mg^{2+}$-binding, substrate-binding, and dimer formation-defective triple mutant). Subsequent enolase activity assays revealed that purified rENO H380A mutant protein presented ~45% activity of WT rENO (Fig. 3*A*), but both rENO S42A and rENO TM completely lacked enzymatic activity (Fig. 3*A*).

Next, we constructed binary vectors expressing WT or activity-deficient ENO mutant proteins fused with a HA-tag at their C-terminus for complementation assay. *Agrobacterium* carrying BaMV and ENO WT or mutant variants were mixed in a 1:1 ratio and infiltrated into GFP- and ENO-silenced leaves at 7 dpa. Protein blots revealed that levels of ENO protein were indeed reduced by ENO silencing (Fig. 3*B*). As described above (Fig. 2*B*), ENO silencing greatly reduced BaMV levels by 90% (Fig. 3 *C* and *D*, lane 2). However, transient expression of ENO WT restored BaMV levels to ~75% at 7 dpi (Fig. 3 *C* and *D*, lane 3), whereas complementation of ENO S42A, ENO H380A partially recovered BaMV levels to 59% and 46%, respectively (Fig. 3 *C* and *D*, lanes 4 to 5). Complementing ENO TM rarely restored

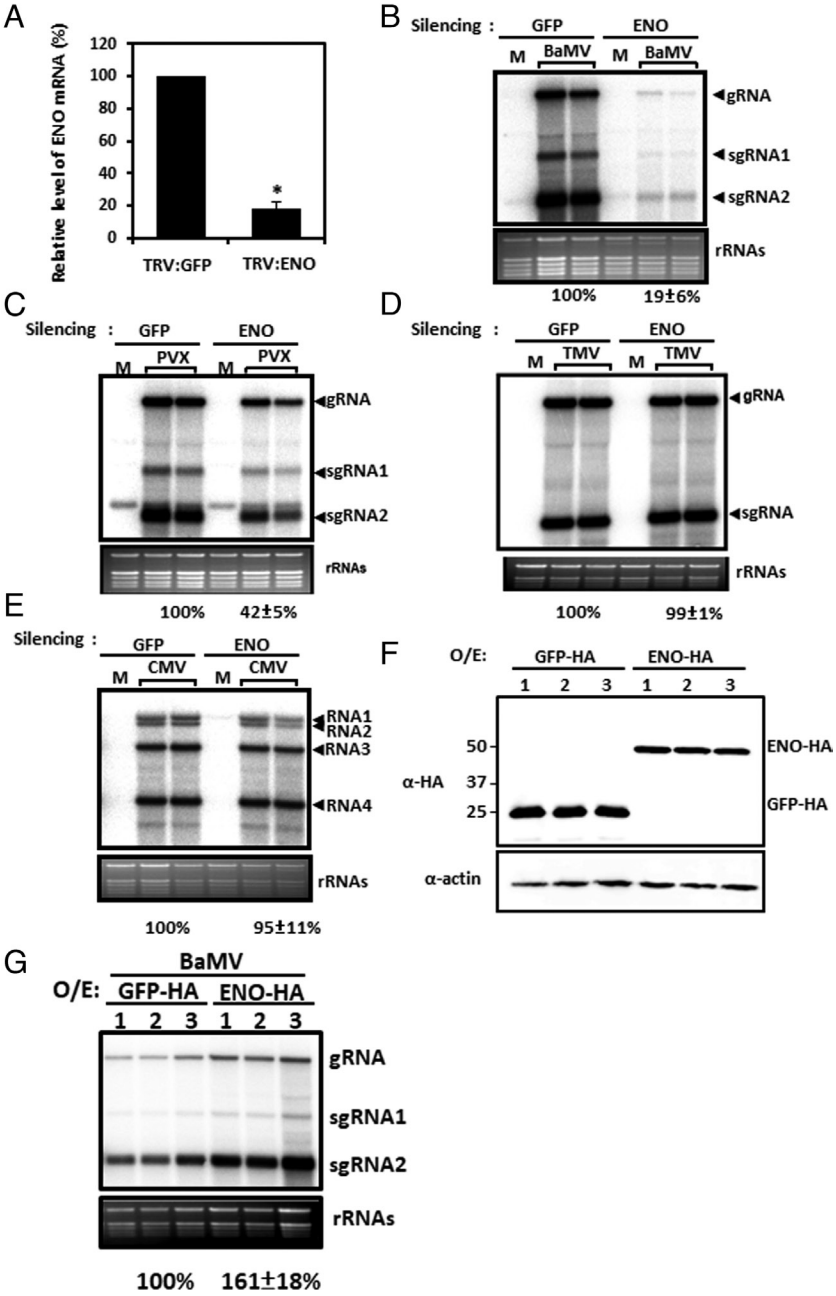


**Fig. 2.** Enolase positively regulates BaMV accumulation. (*A–E*) ENO was silenced using VIGS and GFP-silencing was used as a control. The ENO- or GFP-silenced leaves were harvested at 7 dpa for protoplast isolation followed by virus infection. Protoplasts were harvested at 24 hpi for (*A*) RT-qPCR to quantify ENO levels and RNA blotting to determine (*B*) BaMV, (*C*) PVX, (*D*) TMV and (*E*) CMV infection levels in GFP- and ENO-silenced *N. benthamiana*, respectively. (*F* and *G*) Agrobacterium harboring pKB, and ENO-HA or GFP were mixed at 1:3 ratio and coinfiltrated WT *N. benthamiana* leaves. Infiltrated leaves were harvested at 3 dpi for protein and RNA purification and used for (*F*) ENO-HA expression level by protein blot using anti-HA antibody and (*G*) RNA blot for BaMV detection. TRV: GFP for GFP silencing. TRV: ENO for ENO silencing. M: Mock. BaMV: BaMV-infected. PVX: PVX-infected. TMV: TMV-infected. CMV: CMV-infected. O/E: overexpression.

BaMV levels (Fig. 3 *C* and *D*, lane 6). Under our treatment conditions, all ENO WT and mutant proteins were equally detectable by protein blot analysis using anti-HA antibody in ENO-complemented leaves (Fig. 3*E*), supporting that ENO mutant proteins were successfully expressed and were as stable as ENO WT protein. Together, these findings suggest that the role of ENO in BaMV replication is associated with its enzymatic activity, but nonfunctional ENO, such as ENO S42A, also contributes BaMV replication to some extent.

**ENO's Catalytic Function Is Independent for Its Interaction with $Rep_{BaMV}$.** Although the ENO TM mutant protein failed to complement BaMV replication (Fig. 3), it still displayed similar binding activity to BaMV RNA as ENO WT (*SI Appendix*, Fig. S3*B*). To determine whether the failure of ENO TM to complement BaMV replication was due to its effects on the physical interaction between ENO and $Rep_{BaMV}$, we conducted a ratiometric bimolecular fluorescence complementation (rBiFC) assay to evaluate the interactions of ENO WT and TM proteins binding with $Rep_{BaMV}$ in *N. benthamiana* in vivo. Under confocal microscopy, a YFP signal was observed in the cytosol of *N. benthamiana* leaves infiltrated with *Agrobacterium* carrying pBiFCt-2in1-CN (ENO/$Rep_{BaMV}$) under mock conditions (Fig. 4*A*), indicating that ENO WT can directly interact with $Rep_{BaMV}$ in the absence of BaMV RNA. Moreover, small punctates at the cell periphery, with some dots associated with chloroplasts

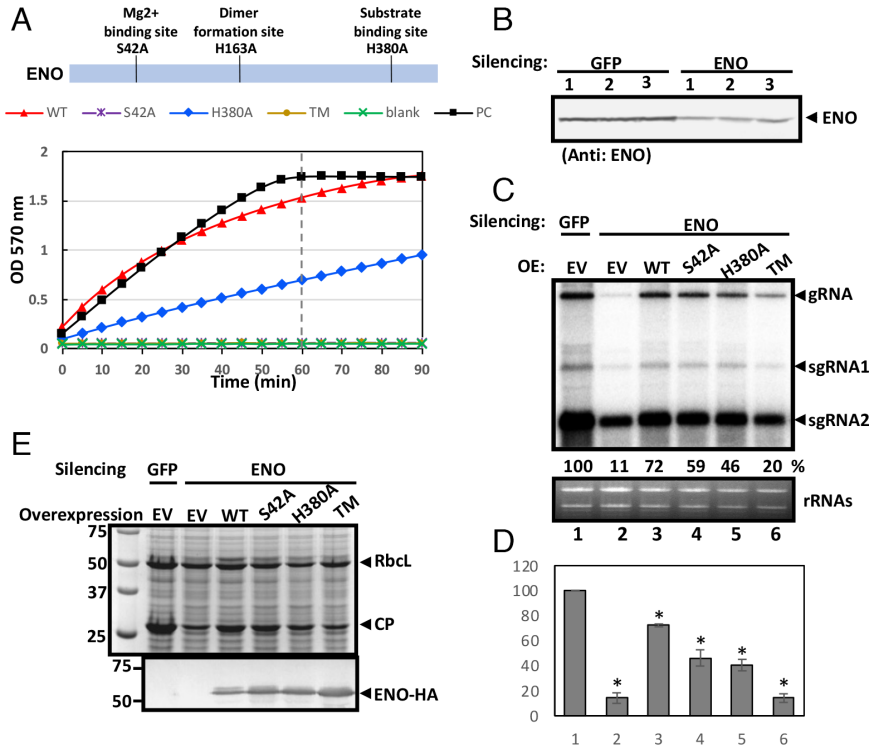


**Fig. 3.** Enolase activity is required for BaMV replication. (*A*) Enolase activity of ENO (WT) and enzymatic deficient mutants. ENO S42A: Ser-to-Ala mutant at the 42nd amino acid (a.a.) in the $Mg^{2+}$ binding site of ENO. ENO H380A: His-to-Ala mutant at the 380th a.a. in the substrate binding site of ENO. ENO TM: S42A, H380A plus H163A (dimer formation site) triple mutant of ENO. PC: positive control. (*B*) Endogenous levels of enolase in GFP- and ENO-silenced *N. benthamiana* at 7 dpa, based on protein blotting using anti-ENO antibody. (*C*) BaMV levels in GFP- and ENO-silenced *N. benthamiana* leaves complemented with ENO WT or mutant variants based on RNA blotting. (*D*) Quantification results of (*C*) by ImageJ analysis from three independent experiments and were used for Student's *t*-test. *$P < 0.05$. (*E*) ENO protein levels of overexpressed ENO WT and enzymatic deficient mutants by Coomassie Blue staining and protein blotting using anti-HA antibody. RbcL: rubisco large-subunit (internal control). EV: empty vector. CP: BaMV coat protein.

were observed in leaves expressing pBiFCt-2in1-CN (ENO/$Rep_{BaMV}$) under BaMV infection (Fig. 4*A*). In contrast, no YFP signal was observed in the leaves expressing pBiFCt-2in1-CN (ENO TM/$Rep_{BaMV}$) (Fig. 4*B*), indicating that the TM mutant lacks the ability to interact with $Rep_{BaMV}$.

To further investigate whether the lack of interaction between $Rep_{BaMV}$ and ENO TM is due to the defect of ENO's enzymatic activity, we performed the rBiFC using a Mg-binding mutant (S42A). As shown in Fig. 4*C*, YFP signals were detected in the leaves expressing pBiFCt-2in1-CN (ENO S42A/$Rep_{BaMV}$), but not in leaves expressing pBiFCt-2in1-CN (EV/$Rep_{BaMV}$). To further confirm these interactions, coimmunoprecipitation assays were performed using ENO-Flag and $Rep_{BaMV}$-HA. Both ENO WT and ENO S42A were successfully precipitated by $Rep_{BaMV}$-HA, while GFP, used as a negative control, was not (Fig. 4*D*). Similarly, when co-expressing pKBRepHA21, an infectious BaMV clone containing an HA-tagged replicase (49), with ENO-Flag or ENO S42A-Flag, the interaction between ENO and $Rep_{BaMV}$-HA also occurred (Fig. 4*E*). In both conditions, ENO S42A showed binding to $Rep_{BaMV}$ comparable to that of WT ENO (Fig. 4 *D* and *E*). These results suggest that the enzymatic activity of ENO is not required for its direct interaction with $Rep_{BaMV}$, either in vivo or in vitro, regardless of the presence of BaMV RNA. However, the inability of the TM mutant to interact with $Rep_{BaMV}$ highlights the essential role of ENO's structural integrity in facilitating this interaction.

**ENO, VDAC, and PYK Colocalize within BaMV VRC Clusters near Chloroplasts and Are Enriched with Mitochondria.** During infection, BaMV hijacks both chPGK (43) and PsbO1 (35) for chloroplast targeting and subgenomic RNA transcription. BaMV infection also induces mitochondrial aggregations and forms a viral complex associated with the mitochondria by interacting with the mitochondrial outer membrane protein, VDAC (38). How BaMV replication is associated with these two autonomous organelles, i.e., chloroplasts and mitochondria, is intriguing. To visualize whether mitochondria and chloroplasts are physically associated with BaMV VRC, we adopted double-stranded RNA (dsRNA) binding protein B2 from *Flock house virus* (50) as an indicator of VRC and transiently overexpressed mito-GFP and B2-OFP in mock- and BaMV-infected *N. benthamiana*. In mock-treated plants, we observed that B2-OFP only resides within the nucleus, whereas mitochondria and chloroplasts were randomly distributed in the cytosol. Some mitochondria formed aggregates around nucleus and few occasionally associated with chloroplasts (Fig. 5*A*). In contrast, large cytosolic B2-OFP clusters with some B2-OFP dots closely associated with mitochondria and chloroplasts were observed in BaMV-infected plants (Fig. 5*A*). These results indicate that BaMV infection induces the formation of cytosolic BaMV VRC clusters along with mitochondrial aggregates and closely associated chloroplasts. Therefore, these two organelles, chloroplasts and mitochondria, and their proteins are also crucial for BaMV replication.

Recent evidence supports that interorganelle communication between chloroplasts and mitochondria relies on a glycolytic and cytosolic PGM-ENO-PYK-VDAC metabolon for both metabolic function and physical interconnectivity (39). Notably, both ENO and VDAC (38) are important HFs for BaMV replication. To elucidate whether glycolytic metabolon-mediated chloroplast-mitochondria associations are involved in BaMV replication, we

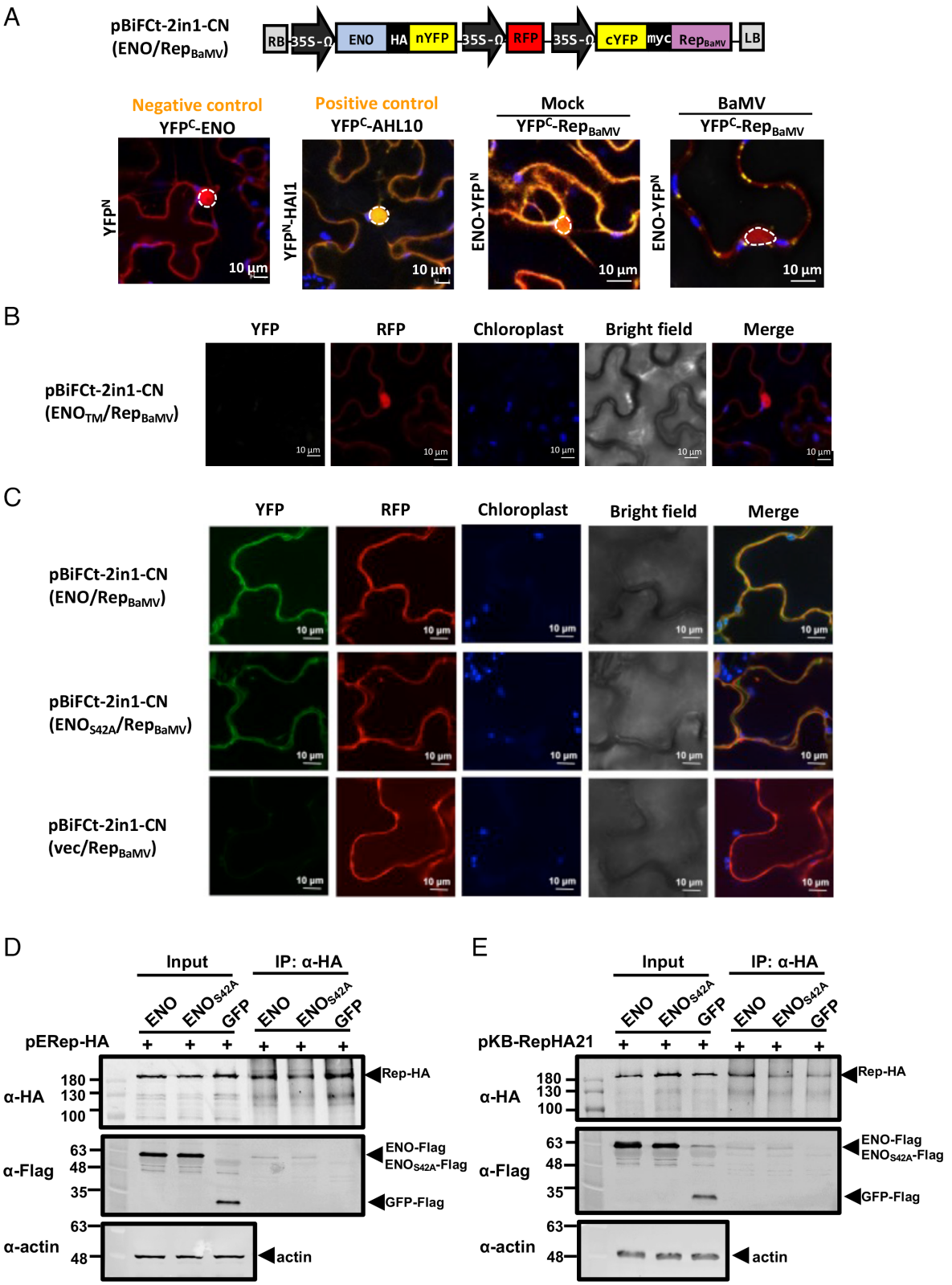


**Fig. 4.** Interaction of ENO WT and mutants with Rep$_{BaMV}$. (*A–C*) rBiFC assay of (*A*) ENO WT, (*B*) ENO TM and (*C*) ENO S42A with Rep$_{BaMV}$. Transient expression of pBiFCt-2in1-CN (ENO WT/Rep$_{BaMV}$), pBiFCt-2in1-CN (ENO TM/Rep$_{BaMV}$), or pBiFCt-2in1-CN (ENO S42A/Rep$_{BaMV}$) in *N. benthamiana* by agroinfiltration. Images of infiltrated leaves were taken at 3 dpa by confocal microscopy. YFP- and RFP-specific fluorescence are shown in yellow and red, respectively. Chloroplast-derived autofluorescence is shown in blue. The dashed circle marks the nucleus. (*D* and *E*) Coimmunoprecipitation assay of ENO WT and mutant with Rep$_{BaMV}$. Transient expression of ENO-Flag, or ENO S42A-Flag, and GFP-Flag with pERep-HA (*D*) or pKB-RepHA21 (*E*) in *N. benthamiana* leaves at 3 dpa. Total protein was extracted and immunoprecipitated using HA antiserum. Following immunoprecipitation, Rep$_{BaMV}$ and ENO were detected by anti-HA and anti-Flag antibodies, respectively. Actin was used as the loading control.

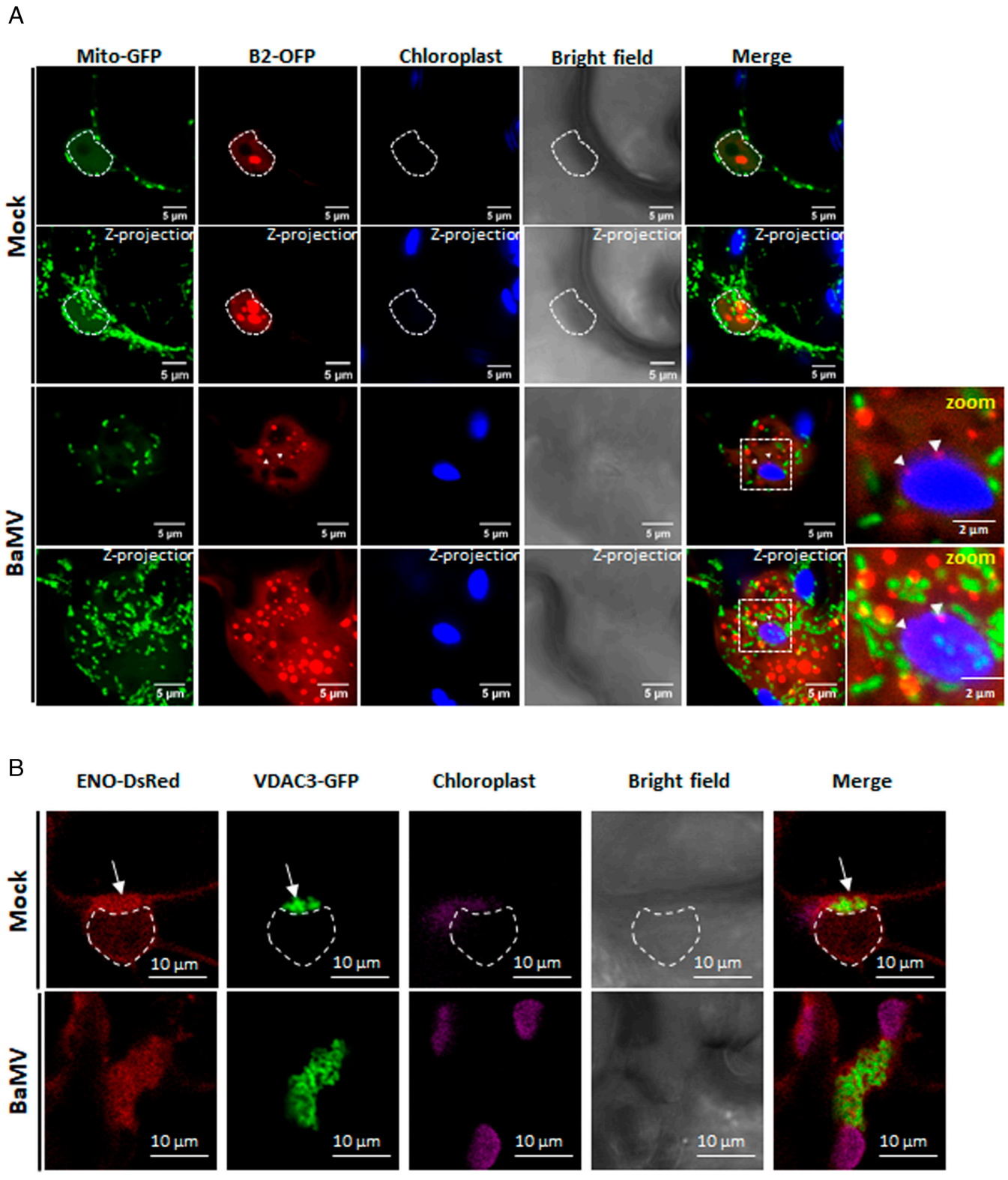


**Fig. 5.** ENO resides in BaMV VRC aggregates associated with mitochondria and chloroplasts. Transient expression of (*A*) mito-GFP and B2-OFP and (*B*) ENO-DsRed and VDAC3-GFP in mock- and BaMV-infected WT *N. benthamiana* at 3 dpa. GFP- and RFP-specific fluorescence is shown in green and red, respectively. The dashed circle indicates the nucleus. Chloroplast-derived autofluorescence is shown in (*A*) blue and (*B*) violet. Filled and empty triangles indicate B2-OFP signal closely associated with chloroplasts and mitochondria, respectively. Arrows indicate B2-OFP signal closely associated with chloroplast. Z-projection images represent computer projections of multiple confocal sections (at least 20 sections per cell, each section approximately 0.5 μm focal depth).

transiently overexpressed ENO-DsRed and VDAC-GFP into mock- and BaMV-infected *N. benthamiana*. We observed that ENO colocalized with overexpressed VDAC aggregates around the nucleus of mock plants (Fig. 5*B*), whereas those ENO- and VDAC-associated aggregates were localized near chloroplasts in BaMV-infected plants at 3 dpa (Fig. 5*B*).

To verify that these large BaMV-induced ENO-VDAC aggregates are associated with BaMV VRC, we adopted bacteriophage

MS2-tagging system to label BaMV viral RNA, along with B2 dsRNA labeling system (50) as an indicator VRC, to visualize BaMV viral RNA and replicating dsRNA in vivo. We agroinfiltrated *N. benthamiana* with pKBsubMS2, an infectious BaMV clone containing eight copies of bacteriophage MS2 CP binding sites (Fig. 6*A*) or pKn and co-expressed $MS2_{FD}$-GFP (51), B2-OFP, and ENO-CFP. In pKn-treated plants at 3 dpa, $MS2_{FD}$-GFP and B2-OFP signals were only observed in the nucleus, $MS2_{FD}$-GFP but not B2-OFP in the nucleolus and ENO-CFP in the cytosol (Fig. 6*B*). However, in MS2-tagged BaMV infected plants, $MS2_{FD}$-GFP formed large aggregates together with ENO-CFP, with some condensed B2-OFP signal embedded inside in cytosol and a few chloroplasts nearby (Fig. 6*B*). By 3D modeling, it clearly showed that B2-OFP signals were surrounded by $MS2_{FD}$-GFP signals and some B2-OFP signals penetrated the chloroplast envelope (Fig. 6*C*). These results demonstrate that ENO, VDAC, and chloroplasts are involved in BaMV VRC clusters.

Considering that the enzymatic function of ENO is important for BaMV replication (Fig. 3), we next tested whether ENO activity plays a role in BaMV VRC formation. ENOblock, a nonsubstrate analogue enolase inhibitor, that binds ENO and modulates its functions, was used to evaluate its effect on BaMV VRC cluster formation. In ENOblock-treated leaves, the size of BaMV VRC clusters and the BaMV titer were significantly reduced compared to DMSO-treated controls (Fig. 6 *D* and *E*). These results suggest that the enzymatic function of ENO is important for the establishment of BaMV VRC and robust replication.

To evaluate whether PYK, another player of PGM-ENO-PYK-VDAC metabolon, also resides in the BaMV VRC, we transiently overexpressed CFP-PYK and ENO-DsRed in mock- or BaMV-infected B2-GFP transgenic *N. benthamiana*. B2-GFP signals in mock-treated plants primarily localized in the nucleus, whereas PYK and ENO colocalized in the cytosol (Fig. 6*E*). However, BaMV infection induced large cytosolic aggregates of B2-GFP that colocalized with CFP-PYK and ENO-DsRed signals in close proximity to chloroplasts (Fig. 6*E*). Taken together, these results demonstrate that ENO, PYK, and VDAC, which are responsible for chloroplast–mitochondria associations, colocalize within the cytosolic BaMV VRC clusters. Importantly, ENO activity also plays a critical role in the formation of BaMV VRC clusters.

**BaMV VRC Includes BaMV Movement Complex.** BaMV infection results in the production of a cytosolic BaMV VRC cluster comprising ER-localized ENO-PYK-VDAC (*SI Appendix*, Fig. S4) and $Rep_{BaMV}$-TGBp1-VDAC-CP (38). Since BaMV movement complex, which includes three TGBps and CP (52), targets to ER, we wondered whether the ER-localized BaMV VRC also contains any BaMV MPs and CP. Thus, we agroinfiltrated B2-GFP transgenic *N. benthamiana* with pKB or pKn and induced coexpression of ER-CFP with TGBp1-mCherry, TGBp2-mCherry, mCherry-TGBp3, or CP-mCherry, respectively.

TGBp1-mCherry was localized in both the nucleus and cytoplasm of mock plants. However, upon BaMV infection, TGBp1-mCherry predominantly colocalized with the BaMV VRC within the ER membrane, and no TGBp1-mCherry signals were detectable in the nucleus. As per a previous report (53), some TGBp1-mCherry puncta were also observed at the cell periphery (*SI Appendix*, Fig. S5).

For ER-localized TGBp2 (54), we observed small TGBp2-mCherry granules in the ER of mock-treated plants, as well as some large aggregates at the cell periphery. After BaMV infection, TGBp2-mCherry was observed within the BaMV VRC at the convoluted ER membrane (*SI Appendix*, Fig. S6).

As reported previously (52), overexpressed mCherry-TGBp3 formed small granules in the ER network of mock-treated plants. However, BaMV infection induced the formation of some mCherry-TGBp3 aggregates in the BaMV VRC associated with the ER membrane, while most mCherry-TGBp3 remained in the ER network (*SI Appendix*, Fig. S7).

CP-mCherry localized in the cytoplasm of pKn-treated plants, but was enriched in the BaMV VRC, with a minor proportion of signal in the cytosol after BaMV infection (*SI Appendix*, Fig. S8). Taken together, our results indicate that the cytosolic BaMV VRC clusters, consisting of viral RNA-$Rep_{BaMV}$-ENO-PYK-VDAC-TGBps-CP, may utilize ER membrane for its intracellular trafficking during infection (*SI Appendix*, Fig. S9).

## Discussion

Viruses utilize membranous structures for replication, often eliciting VRO ultrastructural alterations (1). However, despite BaMV replication and transcription taking place in chloroplasts (35, 43), no obvious modifications of chloroplast morphology have been observed at the ultrastructural level upon BaMV infection. It was reported that mobile cytosolic BaMV VRC aggregates consisting of $Rep_{BaMV}$, TGBp1 and the mitochondrial outer membrane protein VDAC is imbedded in the ER network (38). Therefore, there is a knowledge gap with respect to how chloroplasts, as the BaMV replication organelle, and the mitochondria- and ER-associated cytosolic VRC clusters are interconnected.

In this study, we uncover a positive and essential moonlighting function for ENO in BaMV replication. First, we show that ENO is an RBP to BaMV UTRs with rare affinity to CMV 3′ UTR but not to CMV 5′ UTR (Fig. 1). Second, ENO is critical for BaMV replication, with a minor role in PVX replication and yet no impact on TMV or CMV replication (Figs. 1 and 2). Third, ENO's hydrolase activity amplifies its positive role in BaMV replication (Figs. 3 and 4). Fourth, ENO directly interacts with $Rep_{BaMV}$, and this interaction depends on ENO dimerization rather than its hydrolase activity (Fig. 4). Fifth, BaMV hijacks the ENO-PYK-VDAC metabolon, that is responsible for chloroplast–mitochondrial associations, into BaMV VRC clusters to promote BaMV replication (Figs. 5 and 6). Sixth, ENO enzymatic activity affects the size of BaMV VRC clusters and BaMV accumulation (Fig. 6 *D* and *E*). Therefore, ENO assists BaMV replication possibly through establishing an enzymatically functional metabolon that enhances the physical connection between chloroplasts and mitochondria even though most BaMV RNA and dsRNA replication intermediates are observed in cytosol rather than in chloroplasts (Fig. 6 *B* and *C*). Previously, ENO has been documented as essential for TBSV replication, with its replicase recruiting glycolytic enzymes into its VRC to generate an ATP-enriched compartment beneficial to TBSV replication (8, 10, 55). However, it is worth noting that TBSV is a well-known example of a virus that can replicate in yeast which lacks chloroplasts. Unlike TBSV, BaMV replication requires host factors from both chloroplasts and mitochondria, and these two organelles are enriched within the cytoplasmic BaMV VRC clusters (Fig. 5*A*). Thus, while ENO and other glycolytic enzymes in the TBSV VRO are important for rapid energy supply, the moonlighting function of ENO in BaMV replication may involve maintaining the glycolytic metabolon that dynamically and physically connects chloroplasts and mitochondria. The rapid energy supply and physical connection between chloroplasts and mitochondria, facilitated by glycolytic enzymes, are not mutually exclusive. Further analysis is needed to clarify the role of ENO and other glycolytic enzymes in BaMV replication, specifically in providing a rapid ATP supply.

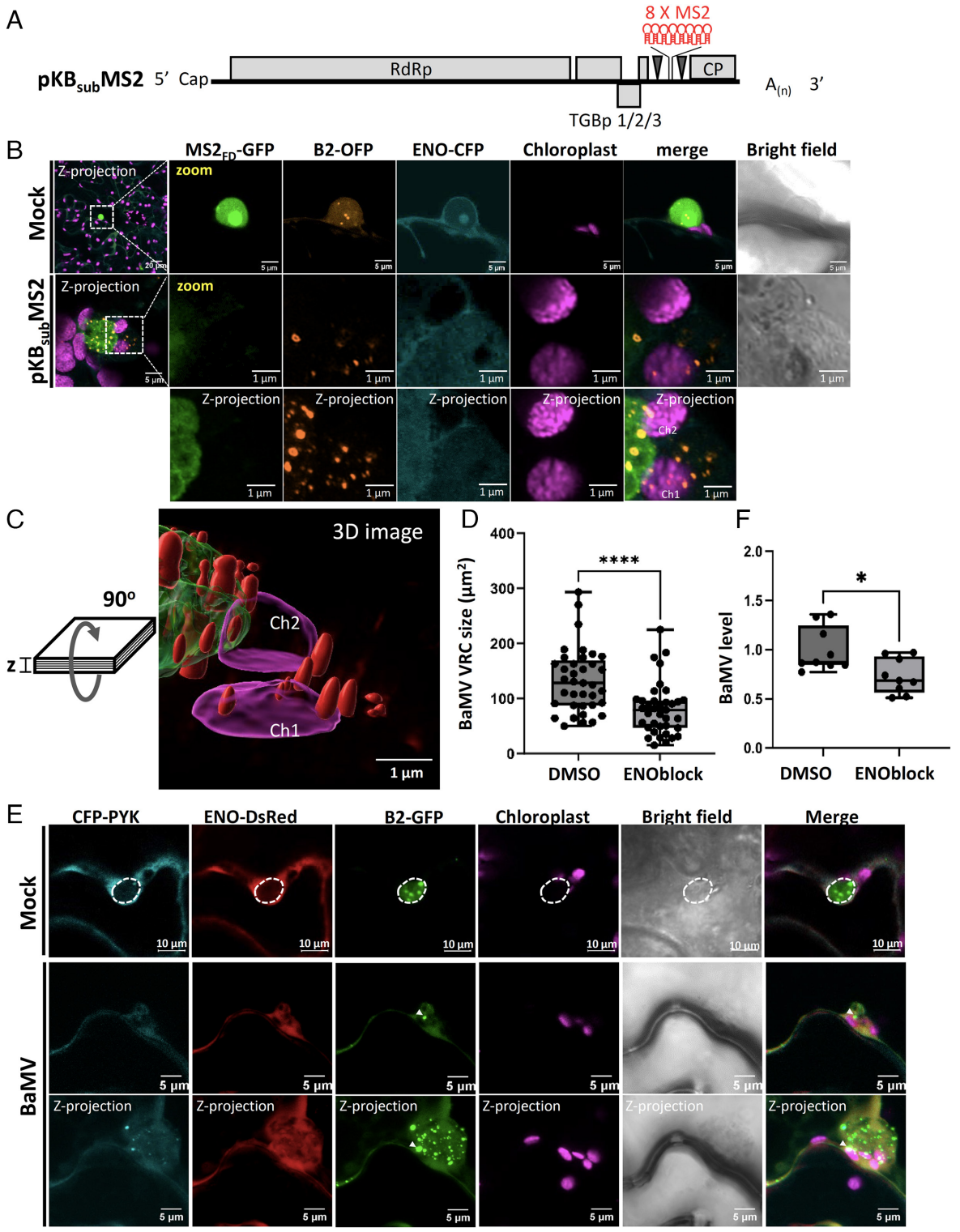


**Fig. 6.** Colocalization of VDAC, ENO, and PYK in BaMV replication complex. (*A*) Schematic representation of the construction of an infectious clone for MS2-tagged BaMV, pKB$_{sub}$MS2. Eight copies of bacteriophage MS2 coat protein binding sequence (8xMS2) were inserted into duplicated subgenomic promoter 2. The triangle represents sgp2. (*B*) Transient expression of MS2$_{FD}$-GFP, B2-OFP, and ENO-CFP with pKn or pKB$_{sub}$MS2 in WT *N. benthamiana.* Images were taken at 3 dpa by confocal microscopy of agro-infiltrated leaves. CFP-, GFP-, and RFP, OFP-specific fluorescence is shown in blue, green, red, and orange, respectively. Chloroplast-derived autofluorescence is shown in violet. Z-projection images represent computer projections of multiple confocal sections (at least 20 sections per cell, each section approximately 0.5 μm focal depth). (*C*) BaMV VRC 3D image by Imaris image analysis software was created from pKBsubMS2-infected sample of *B*. The 3D model was vertically rotated 90 degree. Red represents B2-OFP signal. Violet surfaces were chloroplasts. Green represents BaMV viral RNA. (*D*) The size of BaMV VRC clusters of DMSO and ENOblock treated plants was calculated from Z-projection images. In DMSO and ENOblock treated plants, ten different BaMV-infected cells were selected and the size of BaMV VRC clusters was quantified and used for Student's *t*-test. ****$P < 0.0005$. (*E*) BaMV level in DMSO- and ENOblock-treated plants was quantified by RT-qPCR from three plants, with the experiment repeated three times. Data from three independent experiments were analyzed using Student's *t*-test. *$P < 0.05$. (*F*) Transient expression CFP-PYK, ENO-DsRed, and B2-GFP in mock- and BaMV-infected WT *N. benthamiana* at 3 dpa. Images of agro-infiltrated leaves were taken at 3 dpa by confocal microscopy. CFP-, GFP-, and RFP-specific fluorescence is shown in blue, green, and red or orange, respectively. The dashed circle indicates the nucleus. Chloroplast-derived autofluorescence is shown in violet. The triangle indicates B2-OFP signal closely associated with chloroplast. Z-projection images represent computer projections of multiple confocal sections (at least 20 sections per cell, each section approximately 0.5 μm focal depth).

A glycolytic metabolon associated with the chloroplast TP/PGA transporter has been demonstrated to include host cytosolic PGM, ENO, PYK, and VDAC in the outer mitochondrial membrane (39). This metabolon facilitates the channeling of 2-PG and enables a chloroplast-mitochondria- physical association that is dependent on ENO enzyme activity. Previous studies have shown that chPGK assists in targeting BaMV RNA to chloroplasts during the early replication step (43), while Hsp90 facilitates VRC translocation (42). NbGSTU4 plays a role in counteracting oxidative stress within chloroplasts, thereby promoting efficient viral RNA synthesis (56). Additionally, NbPsbO1, a photosystem II oxygen-evolving complex protein, specifically interacts with the BaMV subgenomic RNA promoter and is essential for efficient sgRNA synthesis (35). BaMV RNA and subgenomic RNAs are likely released from chloroplasts via ATG8- and $Rep_{BaMV}$-enriched vesicles (36). Since ATG8 mediates intrinsic membrane tethering and hemifusion of chloroplasts and ER (57), together with the known action of glycolytic metabolons in connecting chloroplasts and mitochondria (39), we propose that BaMV RNA and the replication complex may release from chloroplasts and hijack ENO, PYK, and VDAC to form large aggregates involving mitochondria, which are surrounded by ER. Thus, BaMV may co-opt host ENO and PYK to connect chloroplasts, where BaMV replication occurs through geometric model and subgenomic transcription. Subsequently, its cytosolic VRC clusters with mitochondrial aggregates to supply energy (38) for robust BaMV replication through stamping models (Figs. 5 and 6). Further, the ER-resident BaMV movement complex consisting of TGBps and CP, which is critical for BaMV intracellular trafficking (28, 52), is also recruited into the cytosolic amorphous BaMV VRC clusters (*SI Appendix*, Figs. S5–S8). The sequential requirement of different intracellular membranous systems for virus replication has also been demonstrated in potyvirus (58, 59). Based on the documented interactions among ENO-$Rep_{BaMV}$, VDAC-$Rep_{BaMV}$, ENO-PYK-VDAC, VDAC-TGBp1 (38), $Rep_{BaMV}$-CP (28), TGBp1-CP, TGBp1-TGBp2, CP-TGBp2, and TGBp2-TGBp3 (52) (*SI Appendix*, Figs. S5–S8 and S9*A*), the compact cytosolic BaMV VRC clusters contain all known proviral HFs, viral proteins, and vRNA, which associate with the ER and traffic along the convoluted ER membrane (*SI Appendix*, Fig. S9*B*). However, unlike PVX TGBp1 that plays a central role in remodeling the ER into X-bodies (60), BaMV TGBps, and CP, when expressed alone, did not elicit any significant disruption or conformational alteration of the host ER network (*SI Appendix*, Figs. S5–S8). Moreover, while BaMV TGBp2 alone formed small granules (*SI Appendix*, Fig. S6), PVX TGBp2 which exerts a dual role in PVX replication and movement (61), induced ER-derived vesicles in the absence of other viral proteins and RNA (62). This difference in VRC formation between BaMV and PVX may explain why ENO has only minor effects on PVX replication but dramatically impacts BaMV (Fig. 2), despite both being potexviruses. Also, the RdRps of related potexviruses, such as PVX and *Plantago asiatica mosaic virus* (PlAMV), contain amphipathic α-helices that mediate membrane binding and multimerization (3, 63). While $Rep_{BaMV}$ appears to contain a putative shorter proline-linked amphipathic α-helix compared to those found in PVX or PlAMV, BaMV replication is known to be associated with intracellular membranes, including perinuclear structures and the ER network (*SI Appendix*, Fig. S4) (38, 43).

We used ENOblock to inhibit ENO function and found that the size of cytosolic BaMV VRC clusters and BaMV titers were significantly reduced by ENOblock (Fig. 6 *D* and *E*). This suggests that suppressing ENO function nullifies the enzymatic functions of metabolon, compromising energy supply and eventually restricting the establishment of cytosolic VRCs and BaMV accumulation. Notably, the enzymatically inactive ENO S42A, but not ENO TM, can partially restore BaMV accumulation in the ENO-knockdown plants (Fig. 3*C*), indicating that both the enzymatic function and structural integrity of glycolytic metabolons are important for BaMV replication. Moreover, we also showed that the subcellular interaction site of ENO and $Rep_{BaMV}$ is affected by BaMV infection, relocating from being evenly distributed in cytosol to forming punctates, some of which are in proximity to chloroplasts (Fig. 4*A*). This indicates that the interaction of ENO and $Rep_{BaMV}$ was concentrated in BaMV VRC during BaMV replication. Binding of ENO to the BaMV UTRs may stabilize the ribonucleoproteins associated with $Rep_{BaMV}$ in the VRC, but this interaction may be irrelevant to the establishment of this glycolytic metabolon. Furthermore, the positive role of ENO in BaMV replication cannot not solely explained by its binding to BaMV UTRs, as the ENO TM can still bind to BaMV 5' UTR but fail to recover BaMV accumulation in ENO-knockdown plants (Fig. 3 and *SI Appendix*, Fig. S3). Considering that the BaMV VRC contains VDAC (38), we propose that BaMV exploits host cell glycolytic metabolons that mediate chloroplast–mitochondrial association to form cytosolic amorphous BaMV VRC clusters. The interaction between ENO-PYK-VDAC and ENO-$Rep_{BaMV}$ is critical for establishment of the clusters.

## Methods

**Plant Materials, Growth Conditions, VIGS.** $Rep_{BaMV}$ transgenic *N. benthamiana* plants were generated by *Agrobacterium tumefaciens* LBA4404 carrying pERep-HA (28) into WT *N. benthamiana* as described previously (64). WT and $Rep_{BaMV}$ transgenic *N. benthamiana* plants (31) were grown in a growth chamber under a 16:8 h light:dark cycle at 25 °C. Fifteen-day-old plants were used for VIGS based on a *Tobacco rattle virus* (TRV) system (65) to knock down specific host genes. *A. tumefaciens* harboring pTRV1 and pTRV2 gene vectors were mixed in a 1:1 ratio and coinfiltrated by syringe onto cotyledons and the first two true leaves of 15-day-old *N. benthamiana*.

**RT-qPCR.** ENO expression and BaMV level were assayed by RT-qPCR using a specific primer set (*SI Appendix*, Table S1) according to a protocol described previously (42). RT-qPCR of Nbactin with specific primers was used as an internal control (*SI Appendix*, Table S1).

**RNA Analysis by Northern Blot Hybridization.** Total RNA was purified by Trizol from infected *N. benthamiana* leaves at 7 dpi and subjected to glyoxylation, before being analyzed by RNA blotting as described previously (44). Specific probes for BaMV, CMV, PVX, and TMV were prepared as described previously (42, 66).

**Enolase Activity Assay.** Recombinant proteins, rENO WT, rENO S42A, rENO H380A, rENO TM, were purified as described previously respectively. 50 ng recombinant proteins of rENO WT and mutants were subjected for enolase activity assay using Enolase assay kit (Abcam) according to the manufacturer's instructions.

**EMSA.** BaMV 5′ UTR and CMV 3′ UTR RNA probes were synthesized by in vitro transcription using T7 RNA polymerase in the presence of α-$^{32}$P-labeled UTP (3,000 Ci/mmol), as described previously (42). Recombinant proteins, rENO WT and rENO TM, were purified as described previously (42) from *Escherichia coli* harboring pET21-ENO and pET21b-ENOTM, respectively. Various amounts of affinity-purified rENO WT and rENO TM were incubated with radioactively labeled RNA probe (4 fmol) in a binding buffer [20 mM Tris-HCl pH 7.9, 20 mM KCl, 10 mM DTT, 5% glycerol, 100 ng yeast tRNA (Sigma), and 2 U of RNase inhibitor] at 30 °C for 20 min. The reaction mixtures were separated on a 5% nondenaturing polyacrylamide gel, and the RNA–protein complexes were detected by a phosphorimager and quantified by ImageJ.

**ENOblock Treatment.** Leaves of 3-wk-old WT *N. benthamiana* were infiltrated with DMSO or 20 μM ENOblock (MedChemExpress, Cat. No.: HY-15858) for 16 h and then agroinfiltrated with agrobacterium carrying pBin61-B2-GFP, pBin-ER-CFP, and pKn or pKB mixed in 1:1:1 ratio for 56 h. The area of cytosolic B2 signals embedded in ER was calculated from the Z-projection images.

**Data, Materials, and Software Availability.** All study data are included in the article and/or *SI Appendix*.

**ACKNOWLEDGMENTS.** We thank Proteomics Core Laboratory, Live-Cell-Imaging Core Laboratory and Genomic Technology Core Laboratory of the Institute of Plant and Microbial Biology, Academia Sinica, Taiwan for technical assistance. This work is supported by grants MOST 107-2313-B-001-012, MOST-108-2313-B-001-005, and MOST 109-2313-B-001-019 from the Ministry of Science and Technology, Taiwan and Academia Sinica Investigator Award, Taiwan.

Author affiliations: [a]Institute of Plant and Microbial Biology, Academia Sinica, Taipei 11529, Taiwan; [b]Graduate Institute of Biotechnology, National Chung Hsing University, Taichung 40227, Taiwan; and [c]Advanced Plant and Food Crop Biotechnology Center, National Chung Hsing University, Taichung 40227, Taiwan

Author contributions: K.-Y.L. and N.-S.L. designed research; K.-Y.L., Y.-W.H., L.-Y.H., H.-C.C., Y.W., I.-H.C., and Y.-P.H. performed research; C.-C.H., C.-H.T., and Y.-H.H. contributed new reagents/analytic tools; K.-Y.L., Y.-W.H., S.-C.L., and N.-S.L. analyzed data; and K.-Y.L. and N.-S.L. wrote the paper.

1. V. Nguyen-Dinh, E. Herker, Ultrastructural features of membranous replication organelles induced by positive-stranded RNA viruses. *Cells* **10**, 2407 (2021).
2. D. Bamunusinghe *et al.*, Analysis of potato virus X replicase and TGBp3 subcellular locations. *Virology* **393**, 272–285 (2009).
3. K. Komatsu *et al.*, Identification of a proline-kinked amphipathic alpha-helix downstream from the methyltransferase domain of a potexvirus replicase and its role in virus replication and perinuclear complex formation. *J. Virol.* **95**, e0190620 (2021).
4. P. D. Nagy, J. Pogany, The dependence of viral RNA replication on co-opted host factors. *Nat. Rev. Microbiol.* **10**, 137–149 (2011).
5. N. Pitzalis, M. Heinlein, The roles of membranes and associated cytoskeleton in plant virus replication and cell-to-cell movement. *J. Exp. Bot.* **69**, 117–132 (2017).
6. I. Fernandez de Castro, J. J. Fernandez, D. Barajas, P. D. Nagy, C. Risco, Three-dimensional imaging of the intracellular assembly of a functional viral RNA replicase complex. *J. Cell Sci.* **130**, 260–268 (2017).
7. N. S. Heaton *et al.*, Dengue virus nonstructural protein 3 redistributes fatty acid synthase to sites of viral replication and increases cellular fatty acid synthesis. *Proc. Natl. Acad. Sci. U.S.A.* **107**, 17345–17350 (2010).
8. M. Molho, C. Chuang, P. D. Nagy, Co-opting of nonATP-generating glycolytic enzymes for TBSV replication. *Virology* **559**, 15–29 (2021).
9. T. S. Huang, P. D. Nagy, Direct inhibition of tombusvirus plus-strand RNA synthesis by a dominant negative mutant of a host metabolic enzyme, glyceraldehyde-3-phosphate dehydrogenase, in yeast and plants. *J. Virol.* **85**, 9090–9102 (2011).
10. R. Y. Wang, P. D. Nagy, Tomato bushy stunt virus co-opts the RNA-binding function of a host metabolic enzyme for viral genomic RNA synthesis. *Cell Host Microbe* **3**, 178–187 (2008).
11. S. Zhao *et al.*, A viral protein promotes host SAMS1 activity and ethylene production for the benefit of virus infection. *Elife* **6**, e27529 (2017).
12. S. Vadlamani, R. Karmakar, A. Kumar, M. S. Rajala, Non-metabolic role of alpha-enolase in virus replication. *Mol. Biol. Rep.* **50**, 1677–1686 (2022), 10.1007/s11033-022-08067-9.
13. N. Kishimoto, N. Iga, K. Yamamoto, N. Takamune, S. Misumi, Virion-incorporated alpha-enolase suppresses the early stage of HIV-1 reverse transcription. *Biochem. Biophys. Res. Commun.* **484**, 278–284 (2017).
14. N. Kishimoto *et al.*, Alpha-enolase in viral target cells suppresses the human immunodeficiency virus type 1 integration. *Retrovirology* **17**, 31 (2020).
15. A. Diaz-Ramos, A. Roig-Borrellas, A. Garcia-Melero, R. Lopez-Alemany, Alpha-Enolase, a multifunctional protein: Its role on pathophysiological situations. *J. Biomed. Biotechnol.* **2012**, 156795 (2012).
16. W. C. Plaxton, The organization and regulation of plant glycolysis. *Annu. Rev. Plant. Physiol. Plant. Mol. Biol.* **47**, 185–214 (1996).
17. D. Xiang-Chun *et al.*, Alpha-enolase regulates hepatitis B virus replication through suppression of the interferon signalling pathway. *J. Viral Hepat* **25**, 289–295 (2018).
18. L. Yang *et al.*, Reduction of the canonical function of a glycolytic enzyme enolase triggers immune responses that further affect metabolism and growth in Arabidopsis. *Plant Cell* **34**, 1745–1767 (2022).
19. N. S. Lin *et al.*, Nucleotide sequence of the genomic RNA of bamboo mosaic potexvirus. *J. Gen. Virol.* **75**, 2513–2518 (1994).
20. Y. I. Li, Y. J. Chen, Y. H. Hsu, M. Meng, Characterization of the AdoMet-dependent guanylyltransferase activity that is associated with the N terminus of bamboo mosaic virus replicase. *J. Virol.* **75**, 782–788 (2001).
21. Y. L. Huang, Y. T. Han, Y. T. Chang, Y. H. Hsu, M. Meng, Critical residues for GTP methylation and formation of the covalent m7GMP-enzyme intermediate in the capping enzyme domain of bamboo mosaic virus. *J. Virol.* **78**, 1271–1280 (2004).
22. Y. I. Li *et al.*, The helicase-like domain of plant potexvirus replicase participates in formation of RNA 5′ cap structure by exhibiting RNA 5′-triphosphatase activity. *J. Virol.* **75**, 12114–12120 (2001).
23. Y. I. Li *et al.*, Identification and characterization of the Escherichia coli-expressed RNA-dependent RNA polymerase of bamboo mosaic virus. *J. Virol.* **72**, 10093–10099 (1998).
24. M. K. Lin, B. Y. Chang, J. T. Liao, N. S. Lin, Y. H. Hsu, Arg-16 and Arg-21 in the N-terminal region of the triple-gene-block protein 1 of Bamboo mosaic virus are essential for virus movement. *J. Gen. Virol.* **85**, 251–259 (2004).
25. M. K. Lin, C. C. Hu, N. S. Lin, B. Y. Chang, Y. H. Hsu, Movement of potexviruses requires species-specific interactions among the cognate triple gene block proteins, as revealed by a trans-complementation assay based on the bamboo mosaic virus satellite RNA-mediated expression system. *J. Gen. Virol.* **87**, 1357–1367 (2006).
26. C. H. Wung *et al.*, Identification of the RNA-binding sites of the triple gene block protein 1 of bamboo mosaic potexvirus. *J. Gen. Virol.* **80**, 1119–1126 (1999).
27. F. DiMaio *et al.*, The molecular basis for flexibility in the flexible filamentous plant viruses. *Nat. Struct. Mol. Biol.* **22**, 642–644 (2015).
28. C. C. Lee *et al.*, The interaction between bamboo mosaic virus replication protein and coat protein is critical for virus movement in plant hosts. *J. Virol.* **85**, 12022–12031 (2011).
29. P. Lan, W. B. Yeh, C. W. Tsai, N. S. Lin, A unique glycine-rich motif at the N-terminal region of Bamboo mosaic virus coat protein is required for symptom expression. *Mol. Plant Microbe Interact.* **23**, 903–914 (2010).
30. Y. P. Huang, I. H. Chen, C. H. Tsai, Host factors in the infection cycle of Bamboo mosaic virus. *Front. Microbiol.* **8**, 437 (2017).
31. C. C. Lee *et al.*, Proliferating cell nuclear antigen suppresses rna replication of Bamboo mosaic virus through an interaction with the viral genome. *J. Virol.* **93**, e00961-19 (2019).
32. I. H. Chen *et al.*, An E3 ubiquitin ligase from Nicotiana benthamiana targets the replicase of Bamboo mosaic virus and restricts its replication. *Mol. Plant Pathol.* **20**, 673–684 (2019).
33. I. H. Chen *et al.*, The function of chloroplast ferredoxin-NADP(+) oxidoreductase positively regulates the accumulation of bamboo mosaic virus in Nicotiana benthamiana. *Mol. Plant Pathol.* **23**, 503–515 (2022).
34. J. W. Lin, M. P. Ding, Y. H. Hsu, C. H. Tsai, Chloroplast phosphoglycerate kinase, a gluconeogenetic enzyme, is required for efficient accumulation of *Bamboo mosaic virus*. *Nucleic Acids Res.* **35**, 424–432 (2007).
35. Y. W. Huang *et al.*, NbPsbO1 interacts specifically with the Bamboo mosaic virus (BaMV) Subgenomic RNA (sgRNA) promoter and is required for efficient BaMV sgRNA transcription. *J. Virol.* **95**, e0083121 (2021).
36. Y. P. Huang *et al.*, Autophagy is involved in assisting the replication of Bamboo mosaic virus in Nicotiana benthamiana. *J. Exp. Bot.* **70**, 4657–4670 (2019).
37. Y. L. Chou *et al.*, The stable association of virion with the triple-gene-block protein 3-based complex of Bamboo mosaic virus. *PLoS Pathog.* **9**, e1003405 (2013).
38. H. C. Lee *et al.*, Voltage-dependent anion channel proteins associate with dynamic Bamboo mosaic virus-induced complexes. *Plant Physiol.* **188**, 1061–1080 (2022).
39. Y. Zhang *et al.*, A moonlighting role for enzymes of glycolysis in the co-localization of mitochondria and chloroplasts. *Nat. Commun.* **11**, 4509 (2020).
40. M. Bachler, R. Schroeder, U. von Ahsen, StreptoTag: A novel method for the isolation of RNA-binding proteins. *RNA* **5**, 1509–1516 (1999).
41. M. Buntru, S. Vogel, H. Spiegel, S. Schillberg, Tobacco BY-2 cell-free lysate: An alternative and highly-productive plant-based in vitro translation system. *BMC Biotechnol.* **14**, 37 (2014).
42. Y. W. Huang *et al.*, Hsp90 interacts specifically with viral RNA and differentially regulates replication initiation of Bamboo mosaic virus and associated satellite RNA. *PLoS Pathog.* **8**, e1002726 (2012).
43. S. F. Cheng, Y. P. Huang, L. H. Chen, Y. H. Hsu, C. H. Tsai, Chloroplast phosphoglycerate kinase is involved in the targeting of Bamboo mosaic virus to chloroplasts in Nicotiana benthamiana plants. *Plant Physiol.* **163**, 1598–1608 (2013).
44. K. R. Prasanth *et al.*, Glyceraldehyde 3-phosphate dehydrogenase negatively regulates the replication of Bamboo mosaic virus and its associated satellite RNA. *J. Virol.* **85**, 8829–8840 (2011).
45. Y. W. Huang, C. C. Hu, N. S. Lin, C. H. Tsai, Y. H. Hsu, In vitro replication of Bamboo mosaic virus satellite RNA. *Virus Res* **136**, 98–106 (2008).
46. C. C. Lee *et al.*, Promotion of bamboo mosaic virus accumulation in Nicotiana benthamiana by 5′->3′ exonuclease NbXRN4. *Front. Microbiol.* **6**, 1508 (2016).
47. M. R. Liou, Y. W. Huang, C. C. Hu, N. S. Lin, Y. H. Hsu, A dual gene-silencing vector system for monocot and dicot plants. *Plant. Biotechnol. J.* **12**, 330–343 (2014).
48. M. A. Troncoso-Ponce *et al.*, Molecular and biochemical characterization of the sunflower (Helianthus annuus L.) cytosolic and plastidial enolases in relation to seed development. *Plant Sci.* **272**, 117–130 (2018).
49. Y. W. Huang, C. C. Hu, C. H. Tsai, N. S. Lin, Y. H. Hsu, Chloroplast Hsp70 isoform is required for age-dependent tissue preference of Bamboo mosaic virus in mature Nicotiana benthamiana leaves. *Mol. Plant Microbe Interact.* **30**, 631–645 (2017).
50. B. Monsion *et al.*, Efficient detection of long dsRNA in vitro and in vivo using the dsRNA binding domain from FHV B2 protein. *Front. Plant Sci.* **9**, 70 (2018).
51. K. R. Luo, N. C. Huang, T. S. Yu, Selective targeting of mobile mRNAs to plasmodesmata for cell-to-cell movement. *Plant Physiol.* **177**, 604–614 (2018).
52. C. H. Wu, S. C. Lee, C. W. Wang, Viral protein targeting to the cortical endoplasmic reticulum is required for cell-cell spreading in plants. *J. Cell Biol.* **193**, 521–535 (2011).
53. Y. W. Huang *et al.*, A viral movement protein co-opts endoplasmic reticulum luminal-binding protein and calreticulin to promote intracellular movement. *Plant Physiol.* **191**, 904–924 (2023).
54. S. C. Lee, C. H. Wu, C. W. Wang, Traffic of a viral movement protein complex to the highly curved tubules of the cortical endoplasmic reticulum. *Traffic* **11**, 912–930 (2010).
55. C. Chuang, K. R. Prasanth, P. D. Nagy, The glycolytic pyruvate kinase is recruited directly into the viral replicase complex to generate ATP for RNA synthesis. *Cell Host Microbe* **22**, 639–652.e7 (2017).
56. I. H. Chen, M. H. Chiu, S. F. Cheng, Y. H. Hsu, C. H. Tsai, The glutathione transferase of Nicotiana benthamiana NbGSTU4 plays a role in regulating the early replication of Bamboo mosaic virus. *New Phytol.* **199**, 749–757 (2013).

57. H. Nakatogawa, Y. Ichimura, Y. Ohsumi, Atg8, a ubiquitin-like protein required for autophagosome formation, mediates membrane tethering and hemifusion. *Cell* **130**, 165–178 (2007).
58. T. Wei *et al.*, Sequential recruitment of the endoplasmic reticulum and chloroplasts for plant potyvirus replication. *J. Virol.* **84**, 799–809 (2010).
59. J. Xie *et al.*, Sugarcane mosaic virus remodels multiple intracellular organelles to form genomic RNA replication sites. *Arch. Virol.* **166**, 1921–1930 (2021).
60. J. Tilsner *et al.*, The TGB1 movement protein of Potato virus X reorganizes actin and endomembranes into the X-body, a viral replication factory. *Plant Physiol.* **158**, 1359–1370 (2012).
61. X. Wu *et al.*, The potato virus X TGBp2 protein plays dual functional roles in viral replication and movement. *J. Virol.* **93**, e01635-18 (2019).
62. H. J. Ju *et al.*, The potato virus X TGBp2 movement protein associates with endoplasmic reticulum-derived vesicles during virus infection. *Plant Physiol.* **138**, 1877–1895 (2005).
63. X. Jiang *et al.*, The N-terminal alpha-helix of Potato virus X-encoded RNA-dependent RNA polymerase is required for membrane association and multimerization. *Viruses* **14**, 1907 (2022).
64. J. F. Topping, Tobacco transformation. *Methods Mol. Biol.* **81**, 365–372 (1998).
65. F. Ratcliff, A. M. Martin-Hernandez, D. C. Baulcombe, Technical Advance. Tobacco rattle virus as a vector for analysis of gene function by silencing. *Plant J.* **25**, 237–245 (2001).
66. K. Y. Lin, Y. H. Hsu, H. C. Chen, N. S. Lin, Transgenic resistance to Bamboo mosaic virus by expression of interfering satellite RNA. *Mol. Plant Pathol.* **14**, 693–707 (2013).